04,12

Electrophysical Properties of Heavy Ion Irradiated PVDF films and PVDF track membranes

© E.A. Volgina[1], N.S. Kirilkin[3], A.N. Nechaev[3], Yu.I. Sotova[2], D.E. Temnov[1]

[1] Herzen State Pedagogical University of Russia,
St. Petersburg, Russia
[2] Military Space Academy named after A.F. Mozhaiskiy district,
St. Petersburg, Russia
[3] Joint Institute for Nuclear Research,
Dubna, Moscow oblast, Russia

E-mail: volgina.elena.1999@mail.ru, detem@yandex.ru

Received November 6, 2025
Revised November 25, 2025
Accepted December 1, 2025

The relaxation and piezoelectric properties of polyvinylidene fluoride (PVDF) films modified by irradiation with heavy ions of Ne, Xe and Bi and subjected to chemical etching are investigated. It has been established that irradiation with ions of different masses leads to a change in the intensity and temperature position of relaxation peaks, which indicates the effect of ion exposure on the segmental mobility of macromolecules. After chemical etching, an additional relaxation process was detected in the region of about $-10\,^{\circ}C$, associated with the formation of a new type of relaxers. It is shown that the effect of a beam of heavy ions causes the appearance of a piezoelectric response, the magnitude of which increases with increasing charge and fluence of the incoming ions. Additional polarization in the negative corona discharge field enhances the piezoelectric response, while chemical etching leads to a decrease in the values of the d_{33} modulus. The results obtained demonstrate a significant effect of the parameters of ion irradiation and subsequent chemical treatment on the relaxation and functional properties of PVDF films.

Keywords: polyvinylidene fluoride, track membranes, ion irradiation, chemical etching, thermally stimulated depolarization current, piezoelectric module.

DOI: 10.61011/PSS.2025.12.63080.314-25

1. Introduction

Polyvinylidene Fluoride (PVDF) is a partially crystalline polymer combining chemical resistance, mechanical strength, and pronounced piezo, ferroelectric, and pyroelectric properties [1–4]. Due to these properties, PVDF is widely used in flexible electronics, sensor devices, implantable medical devices, microelectromechanical systems (MEMS), and filtration systems [5]. The electroactive properties of the material are related to its ability to crystallize in various polymorphic modifications, among which the α- and β-phases play a key role. The nonpolar α-phase, stable under normal conditions, can transform into the polar β-phase under the influence of mechanical stretching, polarization, or irradiation [6–8].

One of the effective methods for modifying the structure and properties of PVDF is irradiation with swift heavy ions (SHI). In this case, narrow cylindrical regions with a disrupted macromolecular structure are formed in the material — latent tracks [9]. Irreversible structural changes occur in these regions: chemical bond breaks, formation of active radicals, and amorphization, accompanied by a decrease in the degree of crystallinity of the polymer [10–14]. The process of chemical etching is accompanied by the diffusion of reagent molecules into the latent track region and the selective destruction of weakened chemical bonds in the polymer matrix [15]. At the same time, along with the expansion of the central part of the track, structural changes occur in the adjacent areas, which can contribute to the formation of new relaxation processes.

It is known that polyvinylidene fluoride occupies an intermediate position between polymers, which are prone mainly to crosslinking, and materials in which destructive processes dominate under the influence of radiation. The nature of the transformations occurring depends significantly on the irradiation conditions, in particular on the ion energy and specific energy losses due to ionization.

One of the key parameters characterizing radiation-induced crosslinking is the gel dose D_g which is a minimum dose at which an insoluble fraction begins to form in the material. Below this value, the crosslinking density is insufficient to form a continuous three-dimensional grid, and the polymer remains completely soluble.

For the β-phase of PVDF, the transition to the gel point upon irradiation with krypton ions (6.2 meV/nucleon) is observed in a wide range of doses — from 9.9 to 35.1 kGy. This variation underscores the significant effect of ionization energy losses on the mechanism of formation of a radiation-induced grid and indicates the complex nature of competing processes of crosslinking and destruction in PVDF.

Relaxation processes in nonradiated PVDF-based films have previously been studied in detail by various methods — mechanical spectroscopy, dielectric spectroscopy [16,17]. The presence of several characteristic relaxation processes has been established. Thus, relaxation near $-40\,^{\circ}$C (α-process) corresponds to vitrification and is associated with dipole relaxation in the amorphous phase. Another process is a α_c-relaxation [18] which is observed in the range of $0-40\,^{\circ}$C and is caused by cooperative dipole-segmental mobility of macromolecules in the interphase region between amorphous and crystalline regions.

In polymer dielectrics, charge accumulation and relaxation are determined by several mechanisms of dielectric relaxation: orientation, interphase, and volume (spatial charge), which manifest themselves at sufficiently high polarizing fields. One of the most informative methods of studying such processes is the method of thermally stimulated depolarization (TSD), which allows us to identify the mechanisms of charge accumulation and relaxation and determine the key energy parameters — activation energy and relaxation times.

This work is devoted to the study of relaxation processes and piezoelectric properties of PVDF films by the method of thermally stimulated depolarization before and after irradiation with heavy ions Ne, Xe and Bi. Special attention is paid to the influence of the nature of ions and subsequent chemical etching of tracks on relaxation parameters and piezoelectric properties. The results obtained make it possible to clarify the mechanisms of dielectric relaxation and the parameters of relaxers in irradiated PVDF films, as well as to determine the optimal conditions for obtaining piezoactive track membranes with improved functional properties.

2. Methods and materials

2.1. Materials

A homopolymer film of polyvinylidene fluoride (degree of crystallinity about 40%) with a thickness of 9 microns of the commercial brand Kureha (Japan) was used in this study. PVDF films were irradiated in cyclotrons IC-100 and U-400 of the Flerov Laboratory of Nuclear Reactions of the Joint Institute for Nuclear Research (Dubna, Russia). Irradiation with ions $22Ne^{+4}$(24 MeV), $132Xe^{+26}$ (158 MeV) and $209Bi^{+51}$(670 MeV) was performed in vacuum at room temperature. The fluence (n) for ions $22Ne^{+4}$ and $209Bi^{+51}$ remained constant on the order of $10^9\,\mathrm{cm}^{-2}$, and ranged from 10^5 to $10^{10}\,\mathrm{cm}^{-2}$ to $132Xe^{+26}$. At these energies, the ranges of ions $22Ne^{+4}$, $132Xe^{+26}$ and $209Bi^{+51}$ for PVDF are 13, 19 and 42 μm, respectively.

Doses absorbed by 9 μm PVDF films, when irradiated with ions Ne (1.2 MeV/nucleon), Xe (1.2 MeV/nucleon) and Bi (3.2 MeV/nucleon) with a flux density of $n = 10^9\,\mathrm{cm}^{-2}$, were 3.9; 10.4 and 186.8 kGy, respectively.

PVDF films irradiated with heavy ions Xe^{26+} with fluence of $10^9\,\mathrm{cm}^{-2}$ and $10^8\,\mathrm{cm}^{-2}$, were etched in an aqueous solution of 10 M KOH and 0.1 m $KMnO_4$ at 65 °C. Then the etched membranes were washed with a solution of $Na_2S_2O_5$ (7.5 % wt.) followed by thorough rinsing in deionized water. Pores of different diameters were obtained by varying the etching time.

The pore sizes were determined by scanning electron microscopy (SEM) using a HITACHI SU8020 microscope.

2.2. Thermally stimulated depolarization current method

Thermally stimulated depolarization current (TDC) measurements were performed in a helium atmosphere using the TSC II installation (Setaram, France). The depolarization current was recorded with a highly sensitive Keithley electrometer with a resolution of up to 10^{-16} A, which ensured high accuracy in measuring low currents.

At the first stage of measurements, PVDF samples were polarized by the contact method at a temperature of 20 °C or 70 °C in an electric field with a voltage of 10 kV/mm for 2 minutes. After polarization, the samples were cooled while maintaining the applied electric field. In the second stage, the polarized sample was heated at a constant rate to a temperature of 70 °C. At the same time, the depolarization current was recorded in continuous mode.

Various methods of processing experimental results were used for the quantitative analysis of relaxation processes, such as the method of varying heating rates [19], the method of activated Eyring states [20] and the method of optimization or numerical modeling of thermodepolarization analysis data [21]. In the latter case, the equation was used for the theoretical calculation of the TSD:

$$j(T) \sim \sum_i \left(S_i \int_0^{\omega_m} \int_0^{W_m} G_i(W, \omega) \times \exp\left[-\frac{W}{kT} - \int_{T_0}^{T} \frac{\omega}{\beta} \exp\left(-\frac{W}{kT'} \right) dT' \right] dW\, d\omega \right) \quad (1)$$

where G_i is the two-dimensional distribution function of relaxers involved in the i-th relaxation process, and S_i is the weighting coefficient of this relaxation process. The criterion for the correctness of determining the parameters of relaxation processes is the most complete coincidence of experimental data and the dependences $I(T)$ calculated using the formula (1), β is the heating rate.

2.3. Method of measuring piezoelectric constants

The piezoelectric module d_{33} was measured using a quasi-static method using a D33 Meter (SinoCera) device. The study was performed for two groups of samples: (1) PVDF films irradiated with heavy ions without subsequent polarization, and (2) films subjected to polarization in the field of a negative corona discharge after irradiation. The polarization was performed at room temperature in an electric field with a voltage of 1 MV/cm for 10 min.

3. Results and discussion

3.1. Irradiated PVDF films

Figures 1 and 2 show the spectra of thermally stimulated depolarization currents for films polarized at temperatures of 20 °C and 70 °C.

At a polarization temperature of 20 °C, two relaxation processes are observed: at −40 °C, the process known from literature data as the PVDF glass transition, and around 25 °C, the α_c-relaxation. 3 relaxation processes are observed when the polarization temperature rises to 70 °C in the temperature range from 0 to 70 °C — in the range of 10 °C, 25 °C and 50 °C.

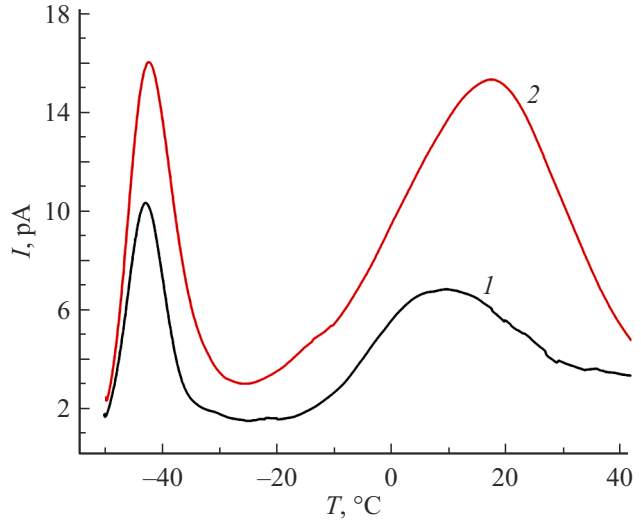

Figure 1. TSD spectra at heating rate $\beta = 6$ °C/min (*1*) and 9 °C/min (*2*) for unirradiated PVDF polarized at $T_p = 20$ °C at $E = 10$ kV/mm

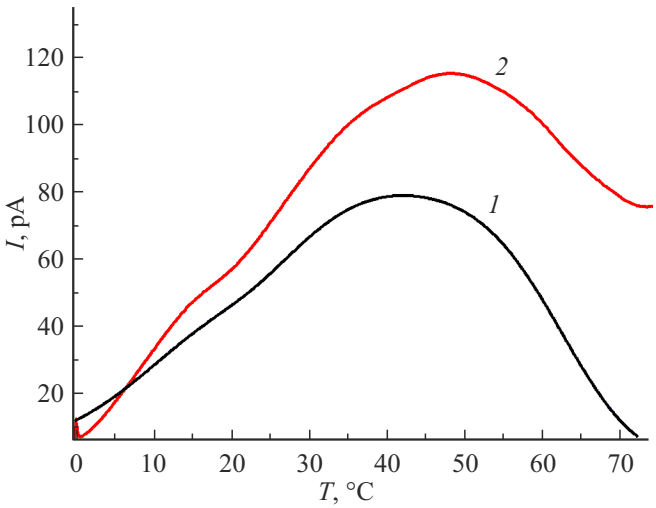

Figure 2. TSD spectra at heating rate of $\beta = 6$ °C/min (*1*) and 9 °C/min (*2*) for unirradiated PVDF polarized at $T_p = 70$ °C at $E = 10$ kV/mm

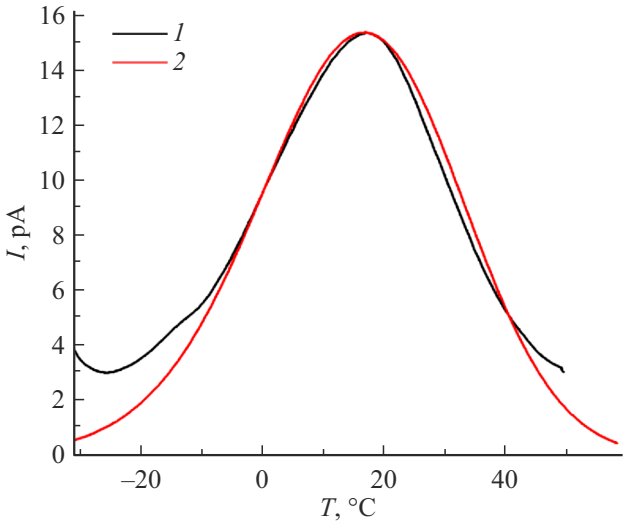

Figure 3. Experimental (*1*) and theoretically calculated (*2*) curve for an unirradiated sample ($T_p = 20$ °C).

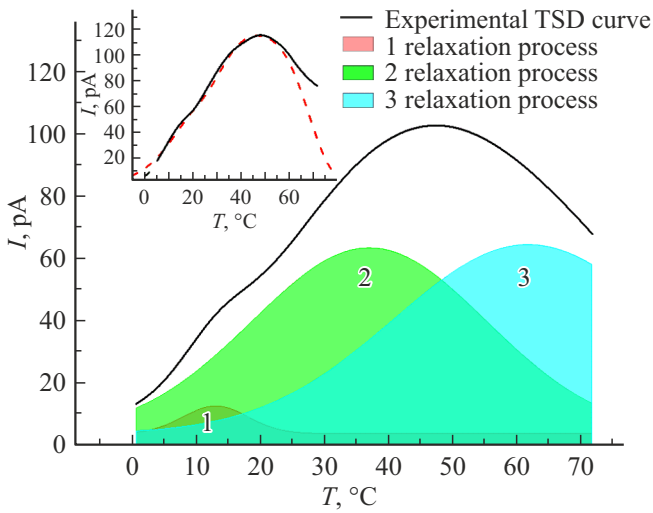

Figure 4. Decomposition of the thermally stimulated current into components responsible for three relaxation processes for an unirradiated sample ($T_p = 70$ °C). The inset shows the correspondence between the experimental TSD curves (solid line) and the theoretically calculated ones (dotted line).

The use of standard methods for processing thermally stimulated current peaks becomes impossible due to the strongly overlapping relaxation processes. The numerical simulation method (optimization method) was used to determine the parameters E_a and α.

Figure 3 shows the coincidence between the experimental and theoretically calculated curve for films polarized at 20 °C. Figure 4 shows the decomposition into 3 components, as well as the coincidence of the experimental and theoretically calculated by the formula (1) a curve with selected parameters of relaxers.

Activation energy of α_c-relaxation (in the region of ~ 25 °C) is 0.64 eV, the corresponding frequency factor is of

Table 1. Values of relaxation parameters in PVDF films polarized at a temperature of 70 °C.

Ion type	1 relaxation process (α_1) (about 10 °C)		2 relaxation process (α_2) (about 25 °C)		3 relaxation process (α_3) (about 50 °C)	
Parameter relaxation process	W_a, eV	ω, s^{-1}	W_a, eV	ω, s^{-1}	W_a, eV	ω, s^{-1}
Unirradiated	0.91	$1.3 \cdot 10^{14}$	0.66	$7.5 \cdot 10^{8}$	0.67	$2 \cdot 10^{8}$

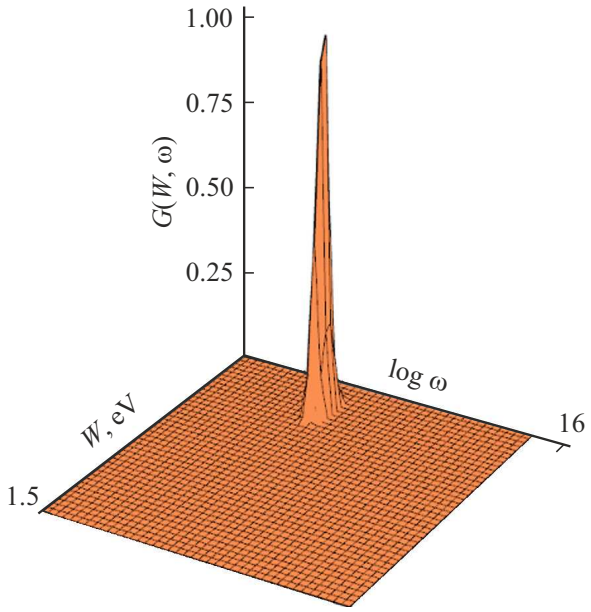

Figure 5. Two-dimensional distribution functions for relaxation processes in PVDF films polarized at 20 °C

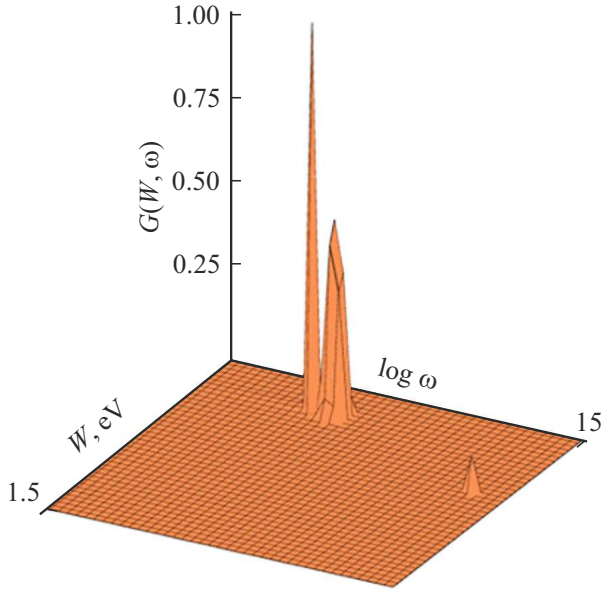

Figure 6. Two-dimensional distribution functions for relaxation processes in PVDF films polarized at 70 °C

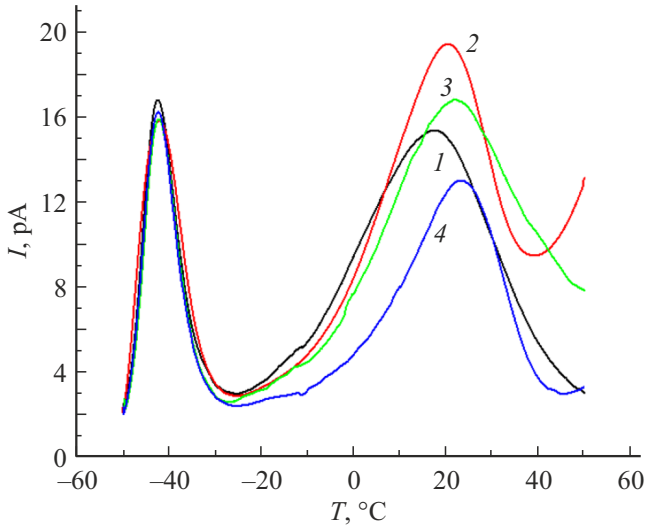

Figure 7. TSD spectra for PVDF film before (*1*) and after irradiation with Ne (*2*), Xe (*3*) and Bi (*4*). Experiment parameters: $E = 10$ kV/mm, $T_p = 20$ °C and $\beta = 9$ °C/min.

the order of 10^8 s^{-1}. In the case of polarization at elevated temperature, the results are presented in Table 1.

Figures 5 and 6 show the final two-dimensional distribution functions of relaxers for the processes observed in irradiated PVDF films.

The effect of irradiation with Ne, Xe, and Bi ions on the relaxation process observed in the region of about 25°C, at a fixed ion flux density of 10^9 cm^{-2} for PVDF films is shown in Figure 7.

It can be seen that an increase in the atomic mass of the bombarding ions leads to a shift of the corresponding relaxation peak to the region of higher temperatures. At the same time, for samples irradiated with Bi ions, in comparison with the unirradiated polymer and films subjected to irradiation with Ne and Xe ions, a decrease in the intensity of this TSD peak is observed.

A decrease in the amplitude of the depolarization current indicates a decrease in the number of active relaxers and a limitation of their mobility, which may indicate the formation of a more rigid and structurally ordered PVDF phase under the influence of heavy ion irradiation.

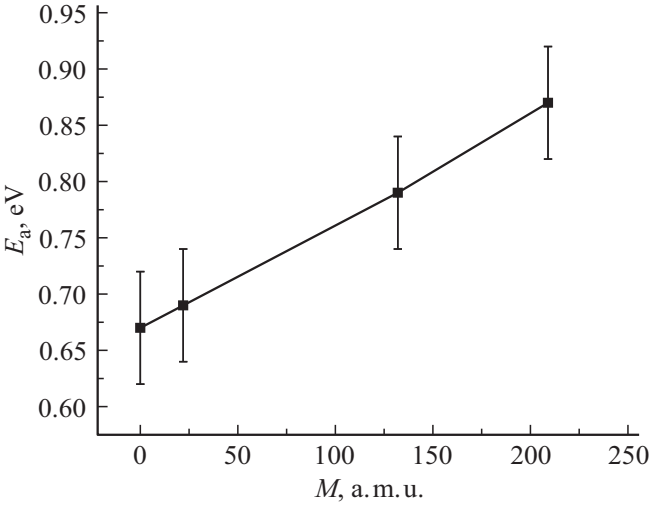

Figure 8. Dependence of the activation energy on the atomic mass of the incoming ions.

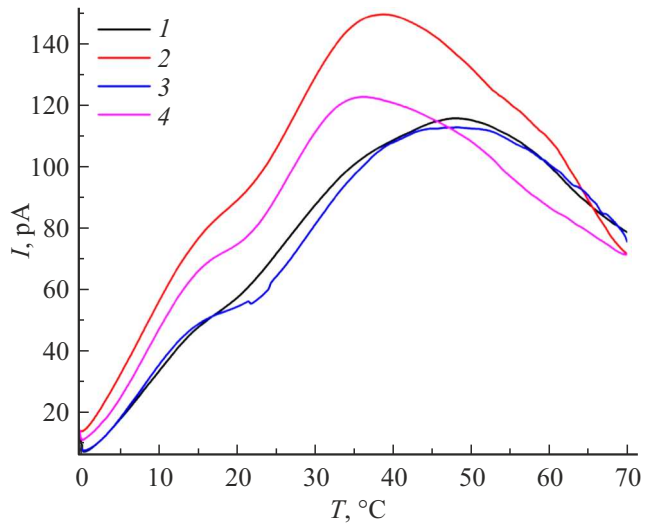

Figure 9. TSD curves for PVDF films: *1* —unirradiated and irradiated *2* — $22Ne^{4+}$, *3* — 132 Xe^{26+} and *4* — $209Bi^{51+}$. Polarization conditions: $T_p = 70\,°C$, $E_p = 10\,kV/mm$ and $\beta = 9\,°C/min$.

The dependence of the activation energy calculated by varying the heating rate on the mass of the incident ion is shown in Figure 8. The frequency factor increases by an order of magnitude as the ion type changes, which may indicate a change in the mass and/or moment of inertia of the relaxers.

At relatively low doses of PVDF radiation, chain destruction prevails, accompanied by an increase in the number of structural defects. The formation of such defects contributes to an increase in the intensity of the depolarization current. As the dose increases to values comparable to D_g, there is a transition to the predominance of crosslinking processes, which leads to difficulty in the mobility of molecular segments, as a result, to an increase in activation energy and a decrease in the intensity of relaxation processes, which is consistent with the experimental data obtained.

An increase in the polarization temperature to 70 °C also allows three relaxation processes in the temperature range from 0 to 70 for irradiated films near 10 °C, 25 °C and 50 °C (Figure 9).

Figure 10 shows the decomposition into three components of the experimental TSD curves for films irradiated with different ions, as well as, in the inset, the coincidence of the experimental curve and the curve theoretically calculated using formula (1) with selected parameters of the relaxators.

Table 2 shows the parameters of the found distribution functions, and Figure 11 shows the two-dimensional distribution functions calculated from them.

The lowest-temperature relaxation process (α_1), observed in the region of about 10 °C, demonstrates significant changes in intensity during the transition from an unirradiated to an irradiated polymer. As can be seen from Figure 10, with an increase in the mass and charge of ions, the intensity of this process increases markedly. This may indicate the development of radiation-induced processes in PVDF.

The relaxation process observed in the region of about 25 °C (α_2) also demonstrates regular changes under the influence of radiation. With an increase in the ion mass, an increase in the activation energy is observed, which is consistent with the previously obtained results identified earlier. As shown in Figure 12, the frequency factor also increases at the same time, which is probably due to the formation of an increasing number of low-molecular defects as the charge and mass of ions interacting with the polymer increase.

For the relaxation process α_3, observed in the region of about 50 °C, the values of the activation energy and frequency factor remain almost unchanged (within the experimental error) for both an unirradiated sample and films irradiated with Ne, Xe, and Bi ions (see Table 2). This process is characterized by a relatively low value of the frequency factor, which is probably due to the participation in relaxation of large fragments of macromolecular chains defrosting at elevated temperatures.

Figure 13, (*a*) and (*b*) show the dependences of the piezoelectric module d_{33} of unpolarized samples on the charge of the incident ion and the fluence of ion irradiation, respectively.

The observed increase in the value of d_{33} with an increase in the charge of the incident ion and fluence may be due to the combined influence of kinetic and thermal effects. The increase in transmitted energy with an increase in the charge of the ion beam contributes to the occurrence of thermal bursts in the volume of the material, accompanied by a short-term local increase in temperature near the ion tracks. This, in turn, causes a temporary softening of the PVDF polymer chains, creating conditions for the orientation of the molecular dipoles along the beam direction.

Table 2. Values of relaxation parameters for heavy ion irradiated PVDF films polarized at a temperature of 70 °C

Ion type	1 relaxation process (α_1) (about 10 °C)		2 relaxation process (α_2) (about 25 °C)		3 relaxation process (α_3) (about 50 °C)	
Parameter relaxation process	W_a, eV	ω, s^{-1}	W_a, eV	ω, s^{-1}	W_a, eV	ω, s^{-1}
$^{22}Ne^{4+}$	0.91	$1.3 \cdot 10^{14}$	0.69	$2.8 \cdot 10^{9}$	0.67	$2 \cdot 10^{8}$
$^{132}Xe^{26+}$	0.90	$1.3 \cdot 10^{14}$	0.78	$7.5 \cdot 10^{10}$	0.67	$2.1 \cdot 10^{8}$
$^{209}Bi^{51+}$	0.91	$1.0 \cdot 10^{14}$	0.84	$8.5 \cdot 10^{11}$	0.67	$2 \cdot 10^{8}$

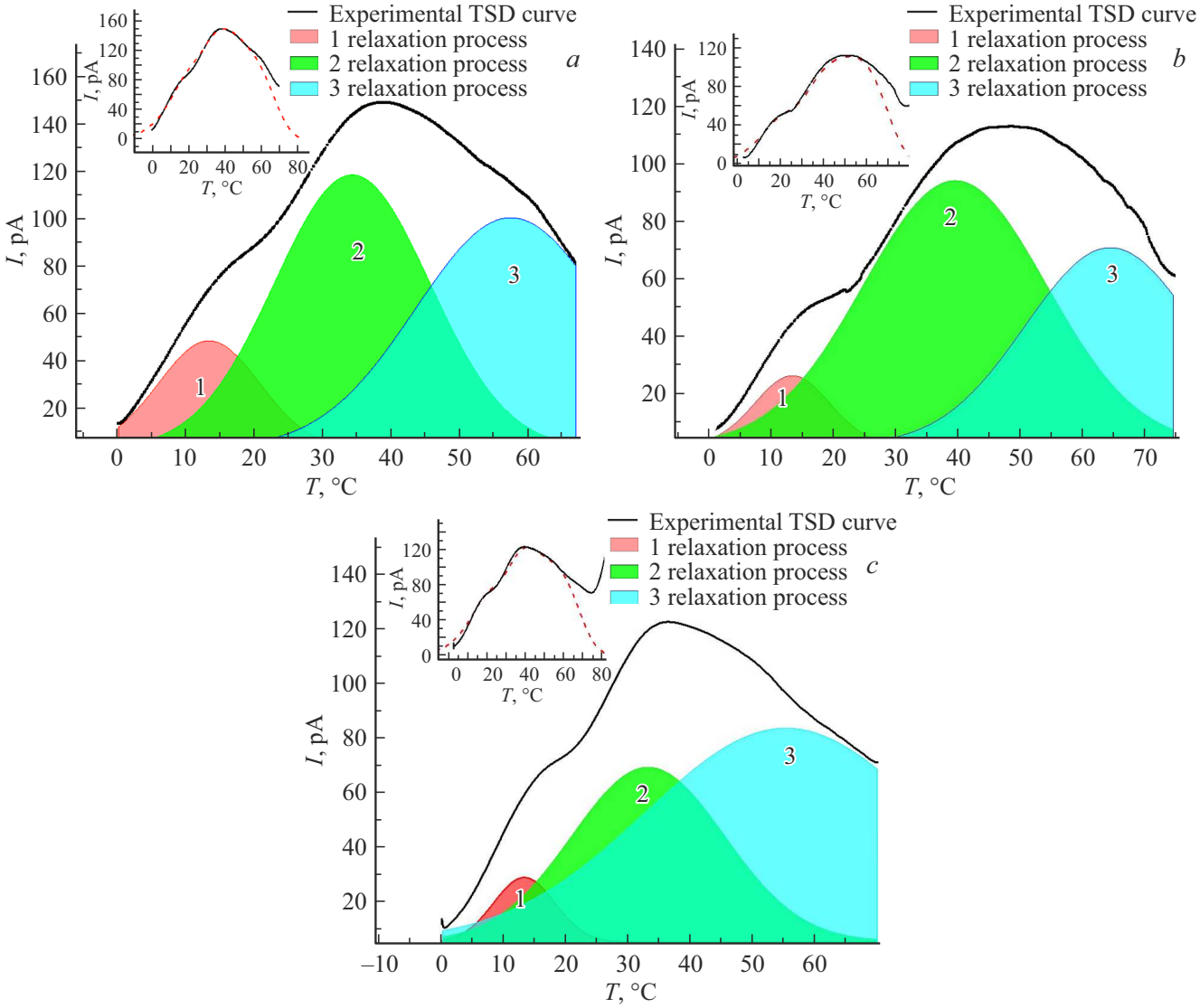

Figure 10. Decomposition of the thermally stimulated current into components responsible for three relaxation processes for: *a* — irradiated with Ne ions, *b* — irradiated with Xe ions, *c* — irradiated with Bi ions. The inset shows the correspondence between the experimental TSD curves (solid line) and the theoretically calculated ones (dotted line).

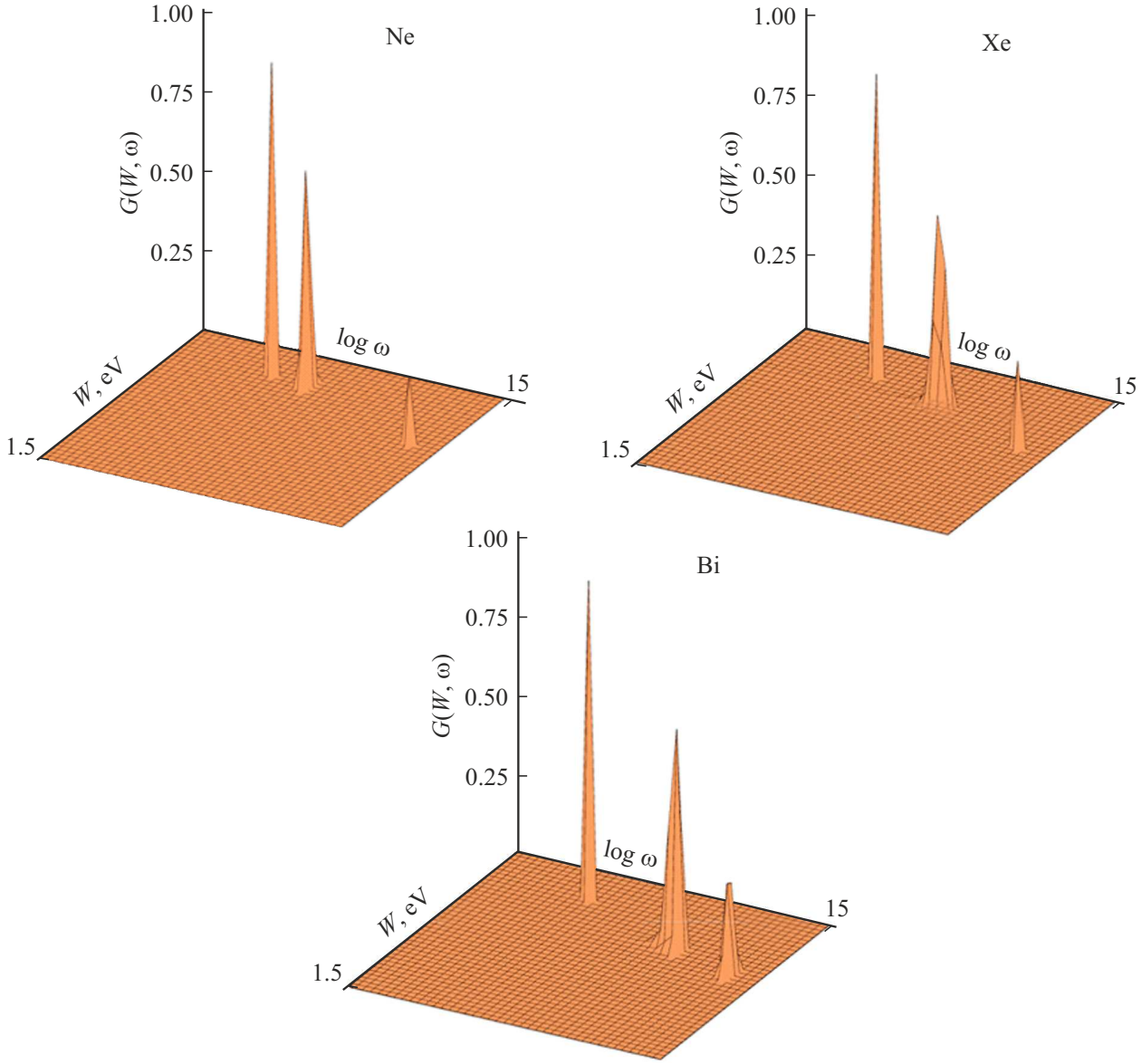

Figure 11. Two-dimensional distribution functions for relaxation processes in films irradiated with Ne ions, Xe ions, and Bi ions.

The additional effect of the polarizing electric field created by the negative corona discharge has an amplifying effect on the formed dipole structures, which is illustrated in Figures 14, (a) and (b). A mutually reinforcing effect is observed for all ions (Ne, Xe, Bi). Thus, we can talk about the synergy effect between irradiation and polarization in the corona discharge.

3.2. Electrophysical properties of PVDF-based track membranes

The etching process involves the penetration of small etchant molecules into the highly depleted core of the track and the selective destruction of chemical bonds. During etching, as the pores grow, new structural defects form in the area of the halo track, which can lead to additional relaxation processes.

Figure 15 shows the spectra of thermally stimulated depolarization current for PVDF films irradiated with Xe ions with fluence 10^8 and $10^9\,\mathrm{cm}^{-2}$ and subjected to subsequent chemical etching of various durations. The process of formation of track membranes, including etching after ion irradiation, is accompanied by the appearance of a new relaxation process observed at a temperature of about $-10\,^{\circ}\mathrm{C}$. This peak is absent in the spectra of samples irradiated with Xe ions but not etched, which confirms its connection with structural changes occurring during track etching.

The appearance of this relaxation maximum is probably due to the appearance of new relaxers forming at the boundary between the latent track walls and the intact

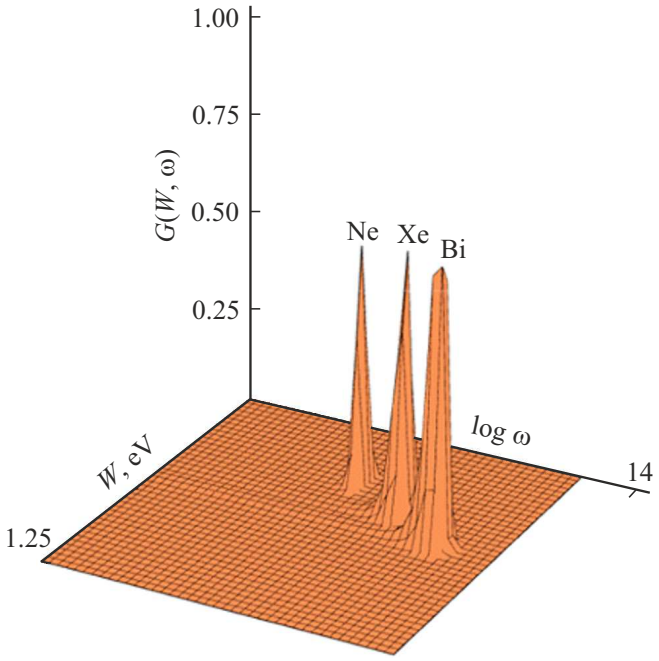

Figure 12. Transformation of the relaxation process observed near 25 °S, with increasing charge and mass of ions.

polymer region. In this case, the peak intensity increases with increasing etching time, which indicates a direct relationship between the number of newly formed relaxers and an increase in the specific surface area of the porous structure.

Studies conducted on PVDF films that were not exposed to ion irradiation, but etched for 15, 45, 60, and 150 min, also revealed the appearance of a weakly pronounced peak in the −10 °C region (Figure 16). However, its intensity is significantly lower than that of the irradiated and then etched samples. This indicates that the etching process itself can cause limited structural modifications of the polymer surface — the formation of defects on the film surface. However, in the absence of latent tracks, these changes are not accompanied by a significant increase in current intensity.

Thus, the occurrence of a pronounced low-temperature relaxation peak under the combined effect of ion irradiation and subsequent etching may be due to the formation of areas of increased defectiveness as a result of irradiation. Upon subsequent etching, these regions transform into interphase zones characterized by increased mobility of macromolecule segments and dipole groups, which leads to the appearance of additional relaxation mechanisms.

An optimization method was used to calculate the activation energy and frequency factor of the process occurring in the −10 °C region. The method of varying the heating rate was used to determine the probable parameters (Figure 17). Figure 18 shows the coincidence of the experimental and theoretically calculated curve for films irradiated with Xe ions with a fluence of 10^9 cm^{-2} and a pore size of 51 nm.

The activation energy of this process was 0.83 eV, and the frequency factor was $2.5 \cdot 10^{12}$ s^{-1}, indicating the presence of highly mobile defective structures. The activation energy of this process does not depend on the etching time and remains constant.

Figure 19 shows a two-dimensional distribution function of relaxers in irradiated PVDF films with subsequent etching.

Figure 20 (*a, b*) shows the dependences of the piezoelectric module d_{33} on the time of chemical etching of PVDF films irradiated with Xe ions at fluence 10^9 cm^{-2}, without polarization in the negative corona discharge field and after it, respectively. A rapid decrease in the value of d_{33} is observed in both cases with the increase of the etching time.

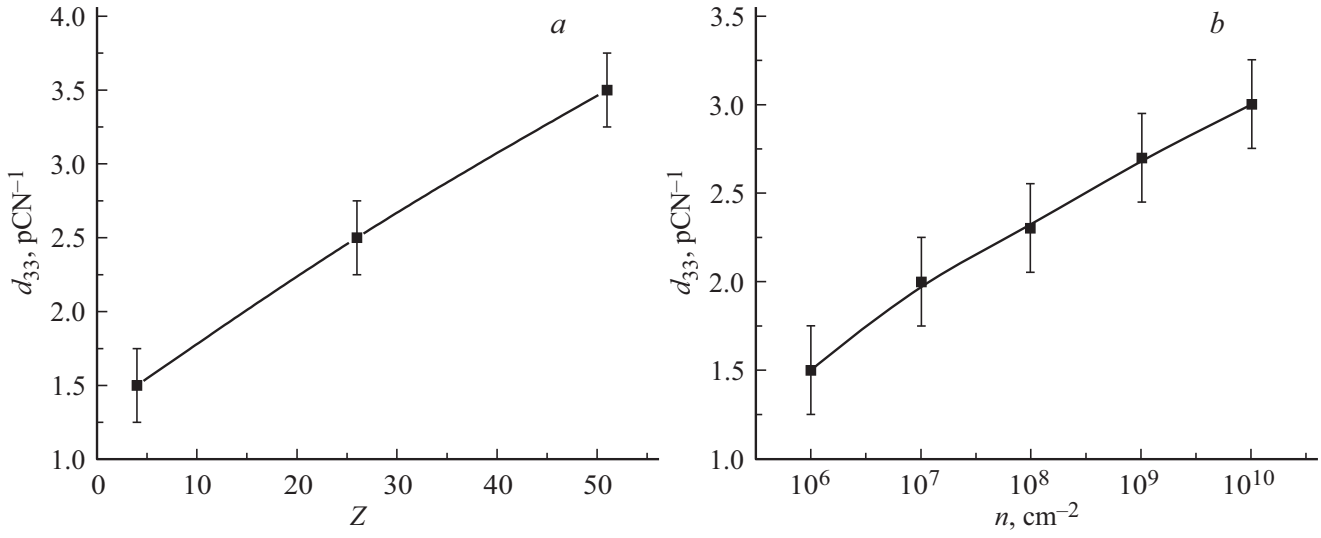

Figure 13. Dependence of the piezoelectric module d_{33}: *a* — on the charge of the incident ion; *b* — on the fluence of the Xe ion.

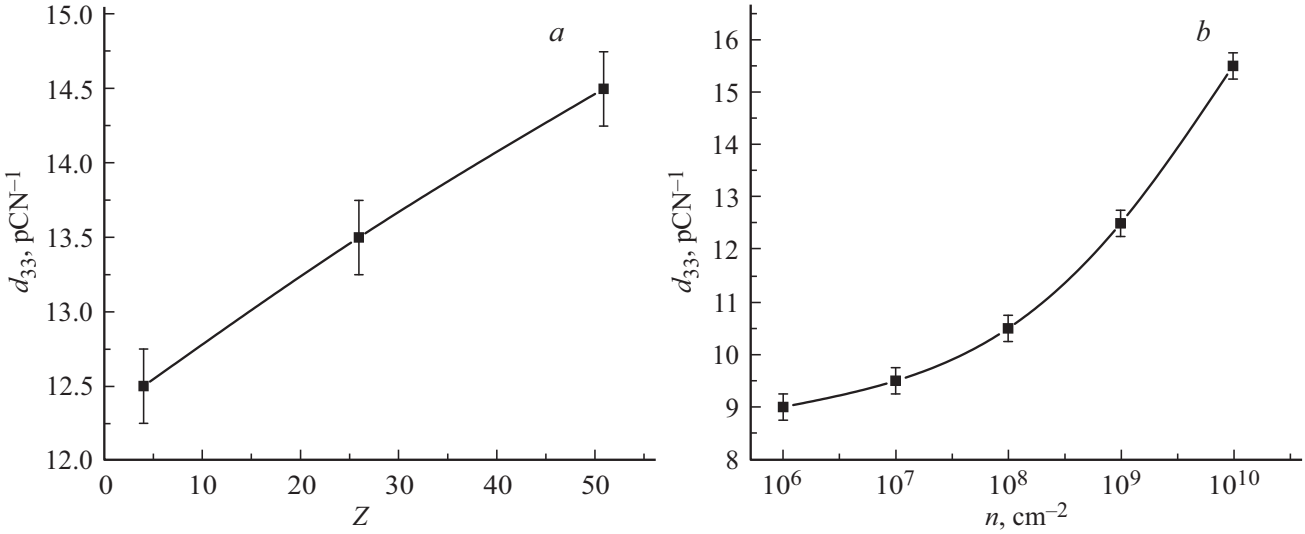

Figure 14. Dependence of the piezoelectric module d_{33} in films polarized in a negative corona discharge: *a* — on the charge of the incident ion; *b* — on the fluence of the Xe ion.

This behavior of the piezoelectric constant indicates the gradual disappearance of the piezoactive phase during chemical etching occurring at elevated temperatures in unpolarized samples. For films polarized in a negative corona discharge, an additional factor in reducing d_{33} may be an increase in surface conductivity as the etching time increases, as well as a decrease in the volume of the polymer matrix due to pore expansion.

It is assumed that the polarized β-phase regions are predominantly localized near the track boundaries and are destroyed in the early stages of etching, which leads to a reduction in the volume of the piezoactive phase and, as a result, to an exponential decrease in the modulus d_{33}.

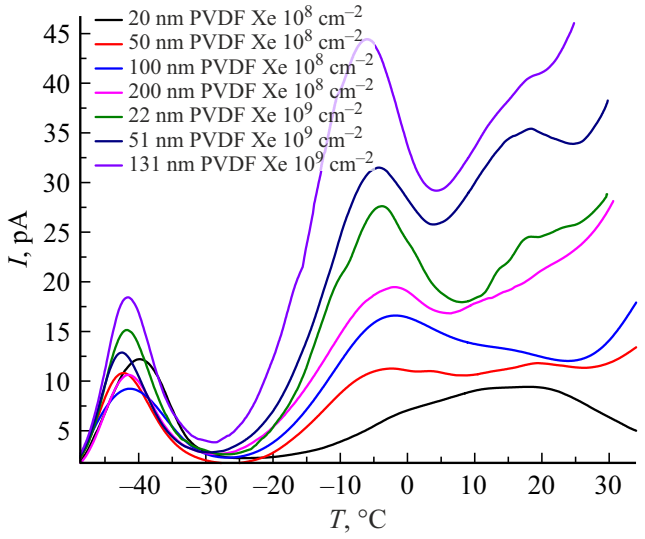

Figure 15. TSD spectra for PVDF films irradiated with Xe ions with a fluence of 10^9 cm^{-2} and 10^8 cm^{-2} with different pore sizes. Experiment parameters: $E = 10$ kV/mm, $T_p = 20$ °C and $\beta = 6$ °C/min.

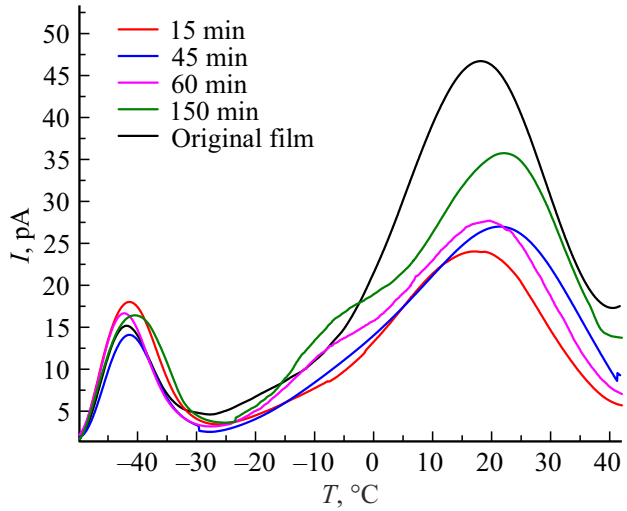

Figure 16. TSD spectra for PVDF film after etching for 15, 45, 60 and 150 min. Experiment parameters: $E = 10$ kV/mm, $T_p = 20$ °C and $\beta = 6$ °C/min.

4. Conclusions

The thermally stimulated depolarization method revealed three cooperative relaxation processes in PVDF films irradiated with heavy Ne, Xe, and Bi ions, which manifest themselves in the temperature range of 0–70 °C. The low-temperature process observed at about 10 °C demonstrates a pronounced dependence of the intensity on the mass and charge of the incoming ions and is caused by the formation of functional groups on the surface and near the tracks,

the concentration of which increases when irradiated with heavier ions. The second, which manifests itself in the region of about 25 °C, is associated with the formation of radiation-induced defects and the processes of crosslinking macromolecular chains, which increase as they approach the gelation point. The high-temperature relaxation process observed near 50 °C is attributable to the increased mobility of large segments of macromolecules in the transition zone between amorphous and crystalline regions.

After chemical etching, an additional relaxation peak was detected in the thermally stimulated depolarization spectra in the region of about −10 °C, associated with the formation of relaxation centers at the pore boundary and near latent tracks. It has been found that the largest number of relaxers occurs precisely in the regions of latent tracks, where defective structures and local inhomogeneities are formed under the influence of ion irradiation, contributing to increased mobility of macromolecule segments. In the samples that were not exposed to radiation, but underwent chemical etching, there is also a weak peak in the same temperature range, which confirms the influence of structural changes caused by exposure to the etchant. However, the significantly higher intensity of this process in irradiated samples indicates the key role of radiation-induced defects in the formation of new types of relaxers at the early stages of etching.

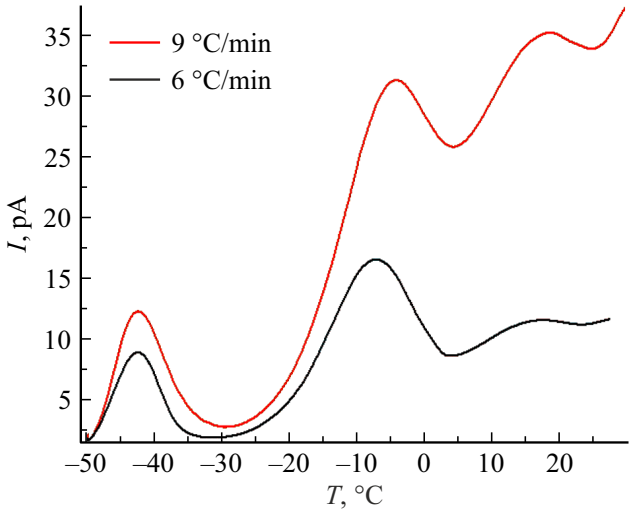

Figure 17. TSD spectra for PVDF-based track membranes irradiated with Xe ions with a fluence of 10^9 cm^{-2} (pore diameter 51 nm). Experiment parameters: $E = 10$ kV/mm, $T_p = 20$ °C.

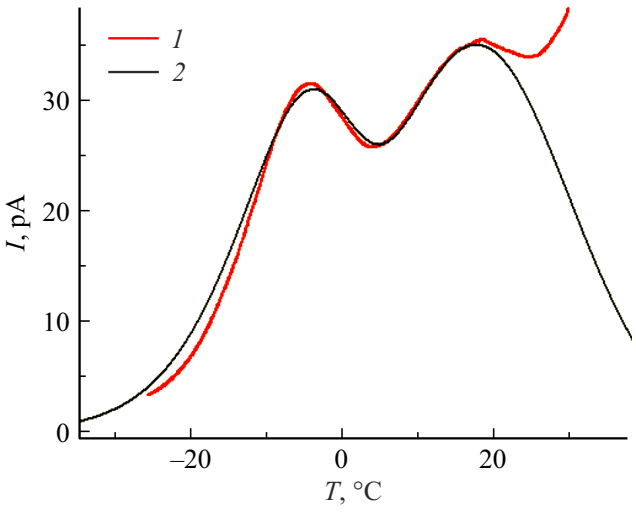

Figure 18. TSD spectra for PVDF-based track membranes with a pore diameter of 51 nm (*1* — practical curve, *2* — theoretically calculated curve).

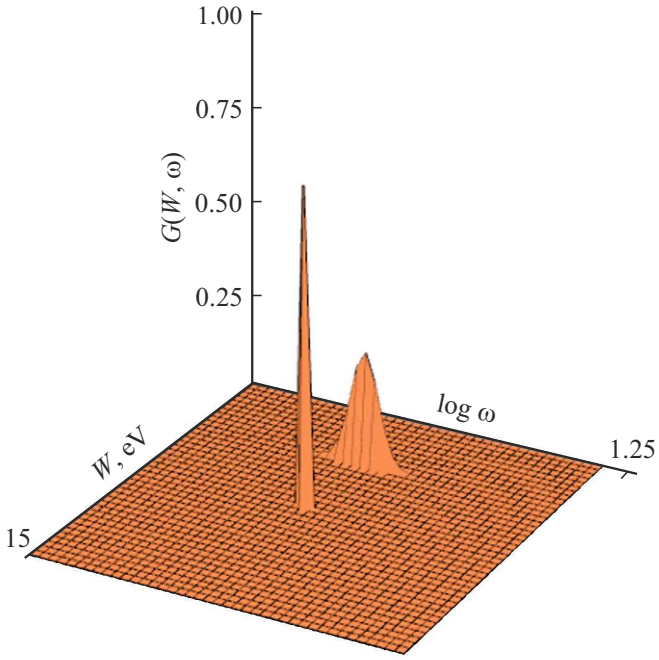

Figure 19. Two-dimensional distribution functions for relaxation processes in PVDF films irradiated with Xe ions with subsequent etching.

Measurements of the piezoelectric module d_{33} have shown that exposure to a beam of heavy ions causes the formation of a stable piezoelectric response, the magnitude of which increases with increasing charge and fluence of the incident ion. The additional polarization in the negative corona discharge field leads to a further increase in d_{33}, which is associated with an increase in the orientation of the dipole groups and an increase in the residual polarization. At the same time, chemical etching is accompanied by a decrease in values of d_{33}, probably due to partial destruction of the polarized regions and changes in conductivity along the tracks, contributing to charge leakage.

Thus, it has been established that the parameters of ion irradiation and subsequent chemical treatment affect the relaxation and functional properties of PVDF films. Control over these parameters makes it possible to purposefully change the structure and piezoelectric characteristics of the

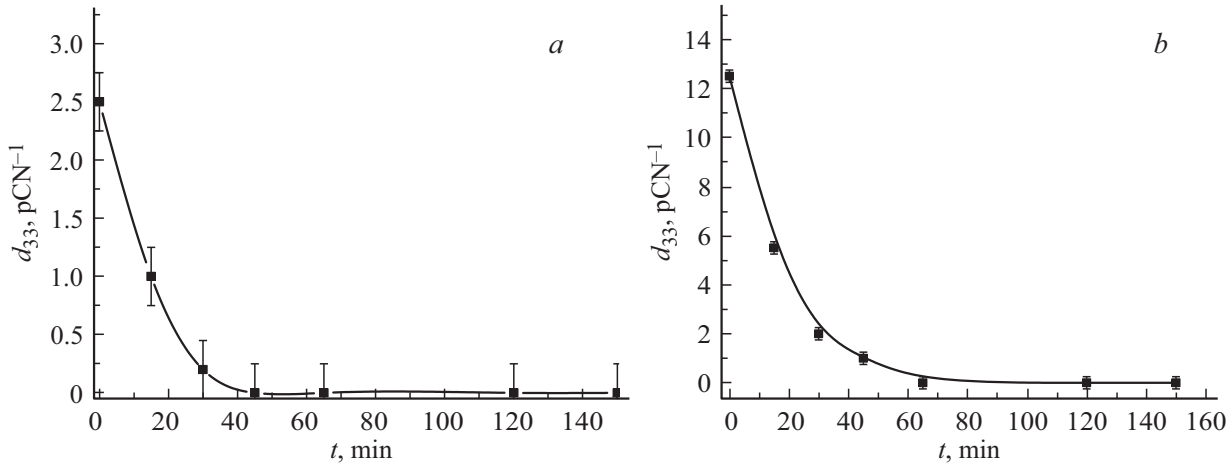

Figure 20. Dependence of the piezoelectric module d_{33} — *a*) on the etching time of a film irradiated with Xe ions with a fluence of 10^9 cm^{-2}; *b*) from the etching time of a film polarized in a negative corona discharge field irradiated with Xe ions with a fluence of 10^9 cm^{-2}.

material, which opens up prospects for its use in new-generation sensor and energy storage devices.

Funding

The research was supported by an internal grant from the Herzen Russian State Pedagogical University (project No. 87-VG).

Conflict of interest

The authors declare that they have no conflict of interest.

References

[1] P. Martins, A.C. Lopes, S. Lanceros-Mendez. Prog. Polym. Sci. **39**, *4*, 683 (2014).
[2] L. Ruan, X. Yao, Y. Chang, L. Zhou, G. Qin, X. Zhang. Polymers **10**, *3*, 228 (2018).
[3] G. Kang, Y. Cao. J. Membr. Sci. **463**, 145 (2014).
[4] C. Ribeiro, V. Sencadas, D.M. Correia, S. Lanceros-Mendez. Colloids Surf., B **136**, 46 (2015).
[5] R. Dallaev, T. Pisarenko, D. Sobola, N. Orudzhev, S. Ramazanov, T. Trčka. Polymers **14**, *22*, 4793 (2022).
[6] A.J. Lovinger, D.D. Davis, R.E. Cais, J.M. Kometani. Polymer **28**, *4*, 617 (1987).
[7] J. Scheinbeim, C. Nakafuku, B.A. Newman, K.D. Pae. J. Appl. Phys. **50**, *7*, 4399 (1979).
[8] V.K. Tiwari, D.K. Avasthi, P. Maiti. ACS Appl. Mater. Interfaces **3**, *5*, 1398 (2011).
[9] R.L. Fleischer, P.B. Price, R.M. Walker. Nuclear Tracks in Solids: Principles and Applications. University of California Press, Berkeley (1975). 605 p.
[10] A. Fina, C. Belin, D. Lesueur, G. Mavel. Nucl. Instrum. Methods Phys. Res., Sect. B, **42**, *1*, 69 (1989).
[11] K. Makuuchi, M. Asano, T. Abe. J. Polym. Sci., Polym. Chem. Ed., **14**, *3*, 617 (1976).
[12] L. Torrisi, G. Foti, Radiat. Eff. Defects Solids, **133**, *4*, 247 (1995).
[13] E. Adem. Radiat. Phys. Chem., **54**, *6*, 637 (1999).
[14] A. Le Bouë dec, N. Betz, S. Esnouf, A. Le Moë l. Nucl. Instrum. Methods Phys. Res., Sect. B, **151**, *1–4*, 89 (1999).
[15] P.Y. Apel, D. Fink, in: D. Fink (Ed.), Transport Processes in Ion Irradiated Polymers, Springer, Berlin, c. 147–202 (2004).
[16] Y. Abe, M. Kakizaki, T. Hideshima. Ferroelectrics **57**, *1*, 9 (1984).
[17] K. Nakagawa, Y. Ishida. J. Polym. Sci., Polym. Phys. Ed. **11**, *8*, 1503 (1973)
[18] E. Volgina, U. Pinaeva, D. Temnov, O. Ivanov, S. Mitrofanov, A. Nechaev. Radiat. Phys. Chem. **230**, 112593 (2025).
[19] A.H. Booth. Can. J. Chem. **32**, *2*, 214 (1954).
[20] S.Z.D. Cheng (Ed.). Handbook of thermal analysis and calorimetry: applications to polymers and plastics. Elsevier, Amsterdam (2002). 714 p.
[21] E. Volgina, D. Temnov, N. Kirilkin, A. Nechaev, A. Rossouw. Radiat. Phys. Chem. **113**, 413 (2025).

Translated by A.Akhtyamov